

# Electrodeposition of Three Dimensionally Ordered Macroporous Germanium from Two Different Ionic Liquids

Jian Hao<sup>1,2</sup>, Jiupeng Zhao<sup>1,4</sup>, Yiwen Zhang<sup>1</sup>, Xiaokun An<sup>1</sup>, Xin Liu<sup>2</sup>,  
Yao Li<sup>2,\*</sup>, and Frank Endres<sup>3,\*</sup>

<sup>1</sup>Center for Composite Material, Harbin Institute of Technology, Harbin, China

<sup>2</sup>School of Chemical Engineering and Technology, Harbin Institute of Technology, 150001, Harbin, China

<sup>3</sup>Clausthal University of Technology, Institute of Electrochemistry, D-38678 Clausthal-Zellerfeld, Germany

<sup>4</sup>State Key Laboratory of Advanced Welding and Joining, Harbin Institute of Technology, 150001, Harbin, China

Three dimensionally ordered macroporous (3DOM) Ge films have been made via ordered polystyrene (PS) templates by electrodeposition from ionic liquids 1-Butyl-3-methylimidazolium bis (trifluoromethylsulfonyl) amide and 1-Ethyl-3-methylimidazolium tris (pentafluoroethyl) trifluorophosphate at room temperature. We discuss the possibility of obtaining high quality 3DOM Ge films from two different ionic liquids by the simple and inexpensive template-assisted electrochemical pathway. Scanning electron microscopy confirms the quality of the samples, and the optical measurements demonstrate that 3DOM Ge made electrochemically shows photonic crystal behavior. Such a material has the potential to make 3DOM Ge feasible for electrical, optical applications and for photonic crystal solar cells.

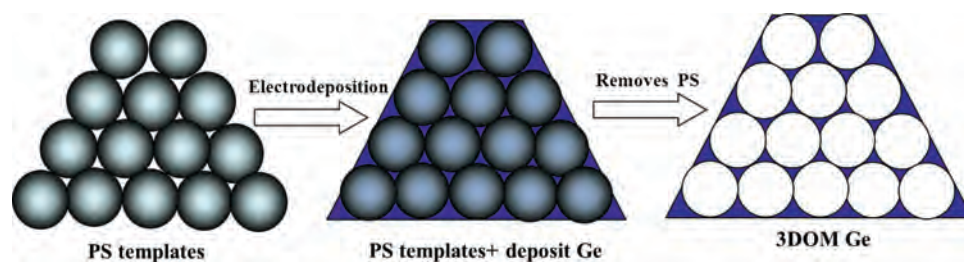
## Keywords:

## 1. INTRODUCTION

Three dimensionally ordered macroporous (3DOM) materials are composed of well interconnected pore and wall structures with wall thicknesses of a few tens of nanometers. Porous solid films have uniform, periodical pores and are ordered in three dimensions.<sup>1,2</sup> They are of potential interest in various fields including lithium-ion batteries,<sup>3,4</sup> solid catalysis,<sup>5</sup> photonic crystal<sup>6</sup> and biochemistry.<sup>7</sup> Especially 3DOM semiconductors are quite promising materials for photonic crystals.<sup>8</sup> A variety of techniques have been used hitherto for the synthesis of 3DOM macroporous materials. Usually, colloidal templates, which are composed of close-packed sub-micrometre monodisperse silica or polymer spheres, are self-assembled and then the interstitial spaces of the templates are infilled with the desired material by using different methods, such as chemical vapor deposition (CVD), chemical deposition, sol-gel techniques and atomic layer deposition (ALD).<sup>9,10</sup> Currently, several 3DOM materials have been synthesised and

investigated including metals,<sup>11</sup> metal oxides,<sup>12</sup> polymers<sup>13</sup> and semiconductors.<sup>14</sup> 3DOM monoliths of hard carbon have been synthesized via a resorcinol-formaldehyde sol-gel process using poly(methyl methacrylate) colloidal-crystal templates by Stein et al.<sup>15</sup> Hector et al. have prepared Ta<sub>3</sub>N<sub>5</sub> on silica substrates by infiltration of such a sol into polystyrene spheres.<sup>16</sup> But sol-gel-based template infilling strategies have a limited use for 3DOM structures due to the defects formed by the volume change. CVD and ALD are both effective methods for the preparation of 3DOM materials. Blanco et al. have successfully fabricated silicon photonic crystals by chemical vapor deposition using Si<sub>2</sub>H<sub>6</sub>, which was first demonstrated by the growth of 3DOM Si using a colloidal crystal template.<sup>17</sup> 3DOM GaP was prepared by ALD using trimethylgallium and tris(dimethylamino)phosphine as precursors for deposition in a SiO<sub>2</sub> colloidal crystal template at 400–500 °C.<sup>18</sup> Both CVD and ALD have similar challenges; usually, any 3D structure which contains narrow interstices cannot be fully filled. Electrophoretic deposition is suitable for introducing preformed nanoparticles into a colloidal

\*Authors to whom correspondence should be addressed.



**Scheme 1.** Schematic illustration of 3DOM Ge films electrodeposited from ionic liquids.

crystal template. Because the deposition occurs in the space between the templates being filled from the bottom of the electrode to the top rather than on the surface of the template spheres, quite a good filling of the structure is feasible. In electrochemical deposition, single or multiple layer of a colloidal crystal template is assembled on a planar surface, which can control the structure of the samples. Electrodeposition techniques are useful for the preparation of conductive polymers,<sup>19</sup> metals<sup>20</sup> and semiconductors.<sup>21</sup>

Germanium is a major material in the optoelectronics industry, as it has the highest dielectric constant ( $\epsilon = 16$ ) and a high refractive index ( $n = 4.12$  at  $\lambda = 2$   $\mu\text{m}$ ), making it a very promising candidate for photonic applications in the IR spectral range.<sup>22</sup> 3DOM germanium are the best materials for photonic crystals. However, the precursors  $\text{GeX}_4$  ( $X = \text{Cl}, \text{Br}$ ) used for the electrodeposition of germanium will hydrolyse rapidly in the presence of water/moisture. Electrodeposition in water is limited to reagents that do not react with water and that can be deposited under conditions where water is not electrolyzed. Ionic liquids have wide electrochemical windows of up to  $\pm 3$  V versus NHE, low vapor pressures, and a good thermal stability, which allows the deposition of semiconductors (such as Si and Ge) that can not be obtained in aqueous solutions. 3DOM  $\text{Ge}$ <sup>23</sup> and 3DOM  $\text{Si}$ <sup>24</sup> have been successfully made by electrodeposition from ionic liquids.

In this paper, we have successfully synthesized 3DOM Ge by multilayer polystyrene (PS) template-assisted electrodeposition at room temperature from the ionic liquids 1-Butyl-3-methylimidazolium bis (trifluoromethylsulfonyl) amide ( $[\text{C}_4\text{mim}]\text{TFSA}$ ) and 1-Ethyl-3-methylimidazolium tris (pentafluoroethyl) trifluorophosphate ( $[\text{C}_2\text{mim}]\text{FAP}$ ).  $[\text{C}_2\text{mim}]\text{FAP}$  is electrochemically, more stable than  $[\text{C}_4\text{mim}]\text{TFSA}$ , but it has a higher viscosity and thus a lower mobility of the electroactive species. There is an interesting observation during the electrodeposition process from the two different ionic liquids. At the same condition, we can easily get single and multiple layer porous structures from  $[\text{C}_4\text{mim}]\text{TFSA}$ , whereas we can just get multiple layer porous structures in  $[\text{C}_2\text{mim}]\text{FAP}$ . The influence of water for the electrodeposition process will be shortly discussed.

## 2. EXPERIMENTAL DETAILS

The ionic liquids 1-Butyl-3-methylimidazolium bis (trifluoromethylsulfonyl)amide and 1-Ethyl-3-methylimidazolium tris(pentafluoroethyl) trifluorophosphate were purchased in the highest available quality from Io-Li-Tec and Merck KGaA and used after drying under vacuum at 100 °C to water contents of below 2 ppm.  $\text{GeCl}_4$  (99.9999%) was purchased from Alfa Aesar and used without any further purification. 0.1 mol  $\text{L}^{-1}$   $\text{GeCl}_4/[\text{C}_4\text{mim}]\text{TFSA}$  and 0.1 mol  $\text{L}^{-1}$   $\text{GeCl}_4/[\text{C}_2\text{mim}]\text{FAP}$  were used as electrolytes. Monodisperse PS colloidal spheres with an average diameter of 425 nm were obtained using an emulsifier-free emulsion polymerization technique. ITO with the PS colloidal crystal template on top was used as a working electrode (WE). A copper wire was in contact with the substrate to provide connection to the potentiostat. An Ag wire was used as a quasi-reference electrode, which gave in this work under the applied conditions a sufficiently stable electrode potential. A Pt-ring was used as a counter electrode. The electrochemical cell was made of Teflon and clamped over a Teflon-covered Viton O-ring onto the substrate. In order to avoid any contaminations, the Teflon cell and O-ring were cleaned before use in a mixture of 50:50 vol% of concentrated  $\text{H}_2\text{SO}_4$  and  $\text{H}_2\text{O}_2$  (35%) followed by refluxing in high purity water.

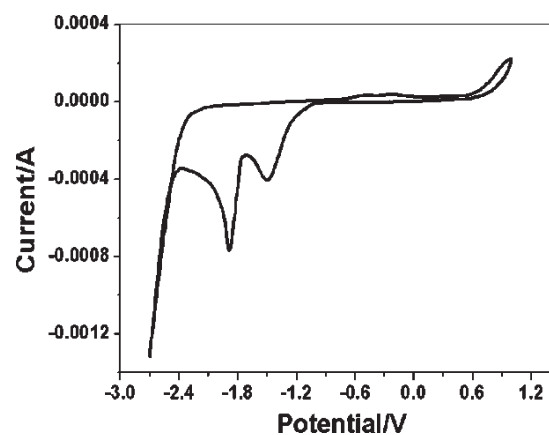


**Figure 1.** Cyclic voltammogram for the electrodeposition of 3DOM Ge from  $[\text{C}_4\text{mim}]\text{TFSA}$ . The scan rate was 10  $\text{mV sec}^{-1}$ .

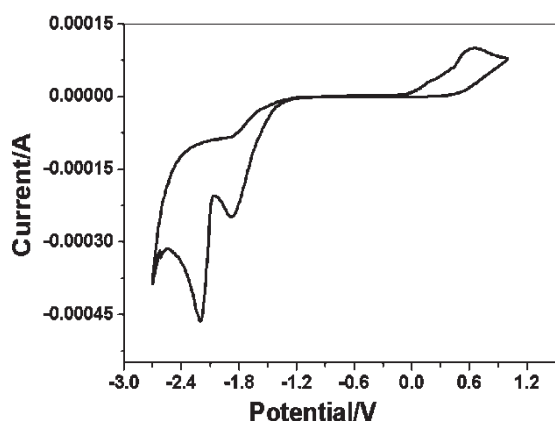


**Figure 2.** Cyclic voltammogram for the electrodeposition of 3DOM Ge from  $[C_2mim]FAP$ . The scan rate was  $10 \text{ mV sec}^{-1}$ .

All electrochemical measurements were performed inside an argon-filled glove box with water and oxygen contents of below 1 ppm. The electrochemical measurements were performed using a VersaStat 2273 (Princeton Applied Research) potentiostat/galvanostat controlled by powerSuite software. Cyclic voltammetry (CV) measurements were performed at a scan rate of  $10 \text{ mV s}^{-1}$  between  $-3.0$  and  $1 \text{ V}$  versus the quasi reference electrode at  $25 \text{ }^\circ\text{C}$ . After the electrodeposition, the deposit was subsequently removed from the glovebox and rinsed quickly in isopropanol to remove the electrolyte. The PS template was removed by tetrahydrofuran (Alfa Aesar), and 3DOM structured films were obtained.

The morphological characterization was performed with a Hitachi S-4800 scanning electron microscope operating at  $20 \text{ kV}$ . The angle resolved reflection spectra of the 3DOM Ge were obtained using Varian Cary 5000 UV-Vis-NIR Spectrophotometer.

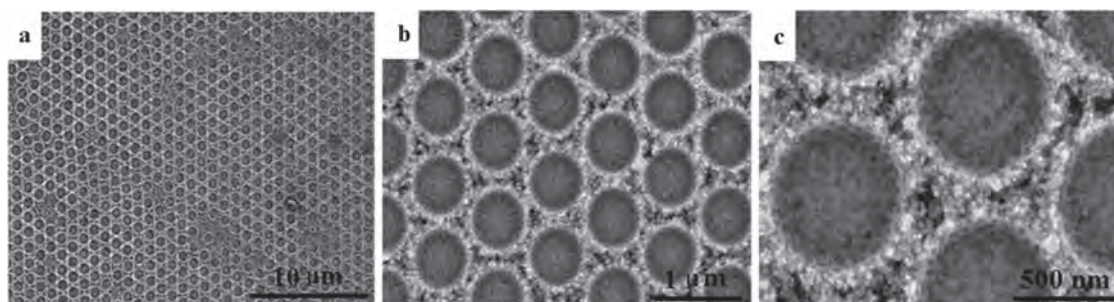
### 3. RESULTS AND DISCUSSION

The fabrication process of 3DOM Ge films is illustrated in Scheme 1. First, the PS templates were prepared by the controlled vertical deposition method. For the vertical self-assembly process of the PS templates, the glass substrates were placed into cylindrical vessels containing a PS latex with a concentration of  $0.1 \text{ vol}\%$ . The vessels were then placed into an incubator at  $65 \text{ }^\circ\text{C}$  to dry for 3–5 days. The

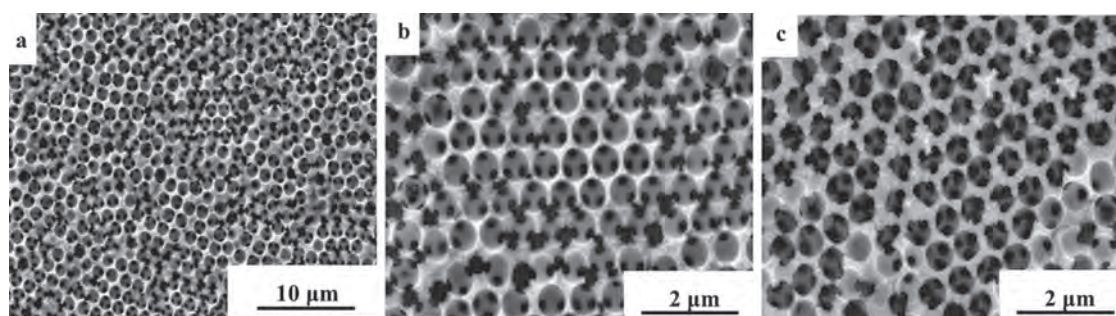
thickness of the colloidal crystal templates can be adjusted via the concentration of the PS latex. Generally,  $0.1 \text{ vol}\%$  PS latex is applied to vertical deposition, templates with 10 layers of PS spheres can be obtained. By this method face centred cubic (FCC) close-packed PS templates with diameter of  $425 \text{ nm}$  are obtained. After electrodeposition, Ge has grown in the empty volume between the spheres, from the bottom up, after removing of the PS spheres, 3DOM Ge films are obtained.

Figure 1 shows the cyclic voltammogram of  $GeCl_4$  in  $[C_4mim]TFSA$  on ITO, covered with a  $425 \text{ nm}$  diameter PS template. There are two main reduction peaks of germanium at potentials of  $-1.5 \text{ V}$  and  $-1.9 \text{ V}$ , corresponding to the reduction of  $Ge(IV)$  to  $Ge(II)$  and of  $Ge(II)$  to  $Ge(0)$ . Figure 2 shows the cyclic voltammogram of  $GeCl_4$  in  $[C_2mim]FAP$  on ITO, covered with a  $425 \text{ nm}$  diameter PS template. There are also two main reduction peaks of germanium at potentials of  $-1.9 \text{ V}$  and  $-2.3 \text{ V}$ , corresponding to the reduction of  $Ge(IV)$  to  $Ge(II)$  and of  $Ge(II)$  to  $Ge(0)$ . The slight shift of the peak position in the two ionic liquid may be due to the quasi reference electrode and the different structure of the ionic liquid/electrode interface. For the purpose of this paper, the focus is set on the electrochemical synthesis of 3DOM Ge and its characterization. Thus, the most suitable deposition potentials of  $-1.9 \text{ V}$  in  $[C_4mim]TFSA$  and  $-2.3 \text{ V}$  in  $[C_2mim]FAP$  were applied for the electrochemical synthesis. A deposition time of 30 min in both ionic liquids was selected. A too long deposition time can lead to dissolution of the deposit in  $[C_4mim]TFSA$ .

Figure 3 shows SEM images of 3DOM Ge films made with PS templates of  $425 \text{ nm}$  diameters. A highly ordered 2-D Ge is made by applying a potential of  $-1.9 \text{ V}$  versus the quasi-reference electrode for 30 min at room temperature in  $[C_4mim]TFSA$ . The obtained 2-D Ge films with a uniform thickness are shown in Figure 3. The thin films left after removal of the PS matrix with THF well retain the ordered, close-packed structure. For the purpose of obtaining 3DOM Ge films, a longer electrodeposition time (1 h) was applied in  $[C_4mim]TFSA$ , but it was seen that the deposit is dissolved with ongoing time, instead of getting 3DOM Ge films at a sufficiently negative electrode potential at room temperature.



**Figure 3.** SEM images of 2DOM Ge from  $[C_4mim]TFSA$  with a little water.



**Figure 4.** SEM images of 3DOM Ge from  $[C_4mim]TFSA$  that was dried prior to use.

It was reported that the electrochemical stability of ionic liquids with the TFSA anion is strongly dependent on the presence of impurities such as water. Therefore, we dried the ionic liquid under vacuum at 100 °C for 24 h to water contents of below 2 ppm.  $[C_4mim]TFSA$  can absorb water easily. Thus, during a long time storage even in the glove box the water content can be increased. After drying, the electrodeposition was done immediately. Figure 4 shows SEM images of 3DOM Ge films made from  $[C_4mim]TFSA$  that was dried immediately before, thus without water. In Figure 4(a), it is seen that the films deposited by this way have only a short range ordering in the larger space; quite in contrast, the films seen in Figures 4(b) and (c) rather show a high ordering in a small

area and the pore walls look disordered as well. This may be due to decomposition of TFSA, and the decomposition products attack the Ge films.  $GeCl_4$  might promote the decomposition of the TFSA anion at the anode.<sup>25</sup>

Figure 5 shows SEM images of a 3DOM Ge layer with a thickness of 1.5  $\mu m$  obtained after applying a constant electrode potential of  $-2.2$  V (versus Ag quasi-reference electrode) in  $[C_2mim]FAP$  for 30 min at room temperature, after removal of the PS spheres with THF. The deposited germanium has a well-ordered macroporous nanoarchitecture consisting of uniform close-packed spherical pores. The holes in the layer below are clearly visible, indicating the three-dimensional ordering of the structure. The smooth surface morphology in Figure 5(a) also shows that

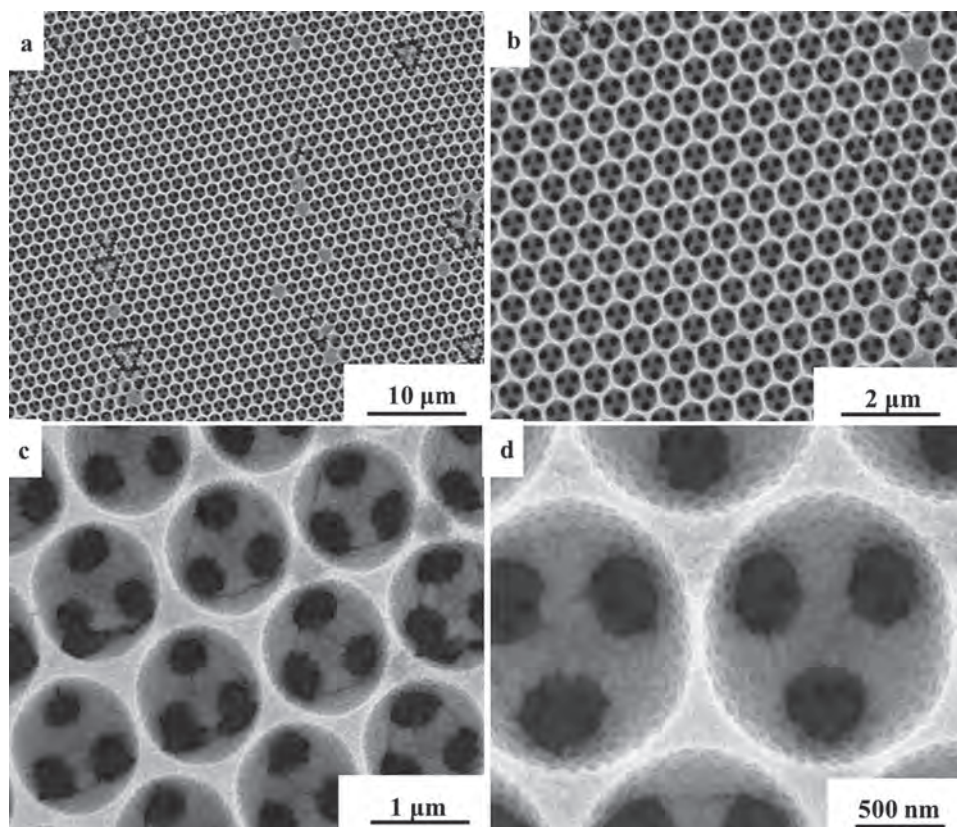


**Figure 5.** SEM images of 3DOM Ge from  $[C_2mim]FAP$ .

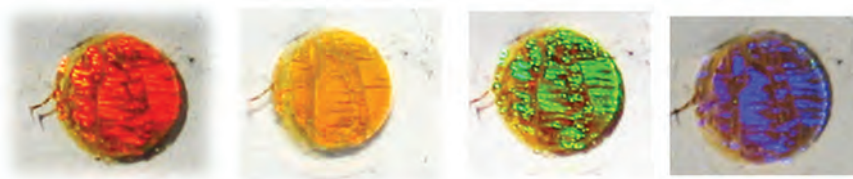


**Figure 6.** Optical photographs of 3DOM Ge on ITO substrate from [C<sub>2</sub>mim]FAP showing a color variation with changing the angle of incident white light.

germanium grows uniformly into the interstices of the PS colloidal crystal template, and the structure is well-ordered on a larger scale. In Figures 5(b) and (c) it is seen that the 3DOM germanium is well ordered. The 3DOM Ge films are composed of nanoparticles (Fig 5(d)), and those nanoparticles are obviously smaller than the ones which are deposited in [C<sub>4</sub>mim]TFSA. The FAP anion is electrochemically more stable. From these observations we can conclude that the choice of the ionic liquid and its water content have a considerable effect on the quality of the 3DOM Ge to be made.

When the incident angle of white light is slightly changed (from 20° – 80°), 3DOM Ge shows reflection colours turning to orange yellow, blue and green (Fig. 6). The colour change of the incident angle is due to Bragg diffraction and a direct evidence for the film's behaviour as a photonic crystal, modulating the incident light. The light reflection of the surface of 3DOM Ge can be explained by Bragg's law,  $2d\sin\theta = n\lambda$  ( $\lambda$  is the wavelength,  $\theta$  is the scattering angle,  $n$  is integer representing the order of the

diffraction peak, and  $d$  is the interplanar distance (centre-to-centre distance of air spheres). Since the refraction effects, the results can be further explained by a combination of Bragg's and Snell's laws,  $\lambda = 2d_{hkl}(n_{\text{eff}}^2 - \sin^2\theta)^{1/2}$ , where  $\theta$  is the angle of the incident to the normal surface;  $n_{\text{eff}}$  is the effective refractive index of the structure, for PS templates,  $n_{\text{eff}} = \sqrt{n_{\text{ps}}^2 f + n_{\text{air}}^2 (1 - f)}$ ,  $f$  is the filling ratio in the FCC structure, = 74.6%;  $d_{hkl}$  is the distance between two diffracting (hkl) planes for the sample.

The function of incident angle of the 3DOM Ge were obtained using Cary 5000 spectrometer, as shown in Figure 7. The result shows that the intensity of the peak at 628 nm, 560 nm and 404 nm increases with the angle. With the same method, we tested another sample obtained [C<sub>2</sub>mim]FAP. Figure 8 reveals that there are three peaks at 628 nm, 560 nm and 402 nm. It can be concluded that the 3DOM materials made electrochemically show photonic crystal behaviour.

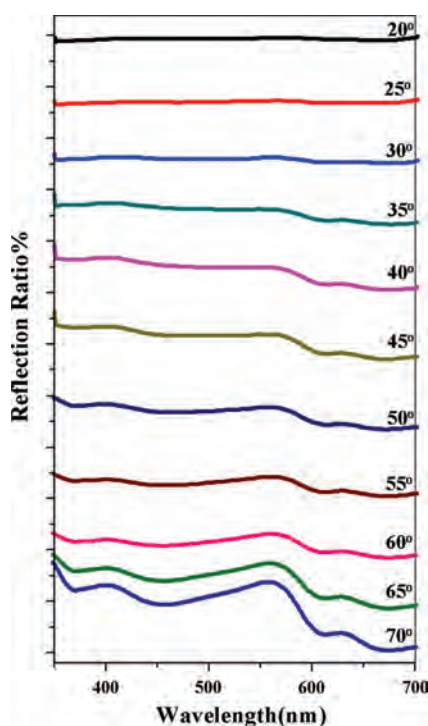


**Figure 7.** Reflection spectra of 3DOM Ge from [C<sub>4</sub>mim]TFSA in the air.

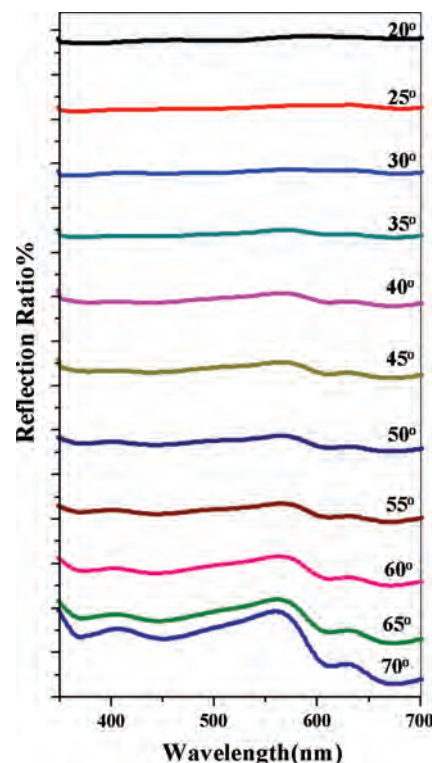


**Figure 8.** Reflection spectra of 3DOM Ge from [C<sub>2</sub>mim]FAP in the air.

#### 4. CONCLUSIONS

3DOM Ge films have been made electrochemically at room temperature by a simple method, which includes self-assembled polystyrene colloidal crystals as templates and the ionic liquid 1-Butyl-3-methylimidazolium bis (trifluoromethylsulfonyl) amide and 1-Ethyl-3-methylimidazolium tris (pentafluoroethyl) trifluorophosphate containing  $\text{GeCl}_4$ . Self-assembled PS colloidal crystals with 425 nm diameter were used as templates. The 3DOM Ge obtained from  $[\text{C}_2\text{mim}]\text{FAP}$  is well-ordered. Water is an important factor to form the 3DOM structure, as with a little water in electrodeposition process, we just can get 2D nanoarchitecture from  $[\text{C}_4\text{mim}]\text{TFSA}$ . The preparation of 3DOM Ge is a relatively simple way for the formation of 3DOM photonic crystals.

**Acknowledgments:** We thank National Natural Science Foundation of China (Nos. 51010005, 90916020, 51174063).

#### References and Notes

1. O. D. Velev, T. A. Jede, R. F. Lobo, and A. M. Lenhoff, *Nature* 389, 447 (1997).
2. J. E. G. J. Wijnhoven, and W. L. Vos, *Science* 281, 802 (1998).
3. M. Hara, H. Nakano, K. Dokko, S. Okuda, A. Kaeriyama, and K. Kanamura, *J. Power Sources* 189, 485 (2009).
4. X. Liu, J. P. Zhao, J. Hao, B. L. Su, and Y. Li, *J. Mater. Chem. A* 1, 15076 (2013).
5. G. Z. Zhang, Z. Zhao, J. Liu, G. Y. Jiang, A. J. Duan, J. X. Zheng, S. L. Chen, and R. X. Zhou, *Chem. Commun.* 46, 457 (2010).
6. K. A. Arpin, M. D. Losego, A. N. Cloud, H. L. Ning, J. Mallek, N. P. Sergeant, L. X. Zhu, Z. F. Yu, B. Kalanyan, G. N. Parsons, G. S. Girolami, J. R. Abelson, S. H. Fan, and P. V. Braun, *Nat. Commun.* 4, 2630 (2013).
7. Y. Q. Teng, Y. Fu, L. L. Xu, B. Lin, Z. C. Wang, Z. A. Xu, L. T. Jin, and W. Zhang, *J. Phys. Chem. B* 116, 11180 (2012).
8. P. V. Braun, *Chem. Mater.* 26, 227 (2013).
9. A. Stein and R. C. Schroden, *Curr. Opin. Solid. St. M.* 5, 553 (2001).
10. A. Stein, B. E. Wilson, and S. G. Rudisill, *Chem. Soc. Rev.* 42, 2763 (2013).
11. H. W. Yan, C. F. Blanford, J. C. Lytle, C. B. Carter, W. H. Smyrl, and A. Stein, *Chem. Mater.* 13, 4314 (2001).
12. M. Sadakane, K. Sasaki, H. Nakamura, T. Yamamoto, W. Ninomiya, and W. Ueda, *Langmuir* 28, 17766 (2012).
13. S. J. Tian, J. J. Wang, U. Jonas, and W. Knoll, *Chem. Mater.* 17, 5726 (2005).
14. A. Esmanski and G. A. Ozin, *Adv. Funct. Mater.* 19, 1999 (2009).
15. K. T. Lee, J. C. Lytle, N. S. Ergang, S. M. Oh, and A. Stein, *Adv. Funct. Mater.* 15, 547 (2005).
16. C. F. Mallinson, B. M. Gray, A. L. Hector, M. A. McLachlan, and J. R. Owen, *Inorg. Chem.* 52, 9994 (2013).
17. A. Blanco, E. Chomski, S. Grachtchak, M. Ibisate, S. John, S. W. Leonard, C. Lopez, F. Meseguer, H. Miguez, J. P. Mondia, G. A. Ozin, O. Toader, and H. M. van Driel, *Nature* 405, 437 (2000).
18. E. Graugnard, V. Chawla, D. Lorang, and C. J. Summers, *Appl. Phys. Lett.* 89, 211102 (2006).
19. D. H. Han, J. W. Kim, and S. M. Park, *J. Phys. Chem. B* 110, 14874 (2006).
20. M. Donten, H. Cesiulis, and Z. Stojek, *Electrochim Acta* 45, 3389 (2000).
21. S. Aksu, J. X. Wang, and B. M. Basol, *Electrochem. Solid St.* 12, D33 (2009).
22. H. Miguez, E. Chomski, F. Garcia-Santamaria, M. Ibisate, S. John, C. Lopez, F. Meseguer, J. P. Mondia, G. A. Ozin, O. Toader, and H. M. van Driel, *Adv. Mater.* 13, 1634 (2001).
23. X. D. Meng, R. Al-Salman, J. P. Zhao, N. Borissenko, Y. Li, and F. Endres, *Angew. Chem. Int. Edit.* 48, 2703 (2009).
24. X. Liu, Y. Zhang, D. Ge, J. Zhao, Y. Li, and F. Endres, *Phys. Chem. Chem. Phys.* 14, 5100 (2012).
25. R. Al-Salman, M. Al Zoubi, and F. Endres, *J. Mol. Liq.* 160, 114 (2011).

Received: 19 May 2014. Accepted: 27 October 2014.